

Proton tunneling in the benzoic acid dimer studied by high resolution ultraviolet spectroscopy

Karen Remmers and W. Leo Meerts

Department of Molecular and Laser Physics, University of Nijmegen, P.O. Box 9010, 6500 GL Nijmegen, The Netherlands

Irving Ozier

Department of Physics and Astronomy, University of British Columbia, 6224 Agricultural Road, Vancouver B.C. V6T 1Z1, Canada

(Received 28 December 1999; accepted 30 March 2000)

High resolution ultraviolet spectroscopy has been used to investigate the rotationally resolved excitation spectrum of the first singlet–singlet transition in the benzoic acid dimer. The measured spectrum consists of two overlapping components. The corresponding lines in the two components are shown to originate in different levels of the ground state potential separated by a tunneling splitting produced by concerted proton exchange between the two subunits forming the dimer. The frequency separation between the two components is equal to the difference between the tunneling splittings in the ground and the excited electronic state. This frequency separation is found to be 1107 ± 7 MHz. From the analysis, it is estimated that the barrier for proton tunneling changes by about 20% upon electronic excitation. The structure of the dimer in the ground state is determined to be linear, while in the excited S_1 state it is slightly bent ($3.4^\circ \pm 1.7^\circ$). © 2000 American Institute of Physics. [S0021-9606(00)01724-4]

I. INTRODUCTION

Hydrogen bonded systems play an important role in many chemical and biological processes. These processes are often governed by proton transfer, which has been extensively studied throughout the last decades. Of special interest is the issue of proton tunneling and how much it contributes to these processes. Carboxylic dimers are well suited systems to study intermolecular proton tunneling since the constituents in these dimers are connected by two intermolecular hydrogen bonds. The displacement of the two protons occurs in concert, and can be described by a single transfer coordinate in a double minimum potential, which is symmetric for an isolated dimer. From infrared measurements, the barrier for proton transfer has been determined to lie between 6400 and 6900 cm^{-1} for both formic acid and acetic acid dimers.¹ Because these barriers are so high, the tunneling splittings are small, and their measurement will require high resolution. Microwave spectroscopy has been used to measure the rotational spectra of several hydrogen bonded bimolecules, two different molecules combined by two intermolecular hydrogen bonds to form an asymmetric polar complex.² Unfortunately, cyclic carboxylic dimers are centrosymmetric, and have no permanent dipole moment. Therefore, they cannot be studied by microwave spectroscopy.

The benzoic acid dimer as well consists of two monomer units connected by two hydrogen bonds. The two hydrogen bonds stabilize the dimer^{3,4} by about 6000 cm^{-1} . Consequently, at low temperatures, only dimers are present. The dimer structure is illustrated in Fig. 1. When the dimer is formed, the structure of the monomers is assumed to remain unchanged. The two monomer units are coplanar. In the ground electronic state, the molecule is linear; that is, the

a -axes of the monomers are colinear. The structure of the dimer can then be characterized by a single distance r , which is here taken to be the distance between the center of mass of the dimer and the center of mass of either monomer unit. The two tautomers of the benzoic acid dimer can be interconverted by concerted proton transfer.

In the description of a general asymmetric proton-transfer potential, it is necessary to introduce two constants, an asymmetry parameter and a tunneling matrix element. The asymmetry parameter is defined to be the energy difference between the lowest level in one potential well and that in the other in the limit that the tunneling matrix element vanishes. The tunneling matrix element couples these two lowest levels, and is defined so that it equals the tunneling splitting in the limit that the asymmetry parameter vanishes.

The benzoic acid dimer has been extensively studied in various condensed phase environments.^{5–21} In these cases, the two benzoic acid units will experience different local environments, and the double-minimum potential will be asymmetric. In the pure benzoic acid crystal,²⁰ the asymmetry parameter is found to be 60 cm^{-1} . Due to the asymmetry, the population at very low temperatures will be highly concentrated in the deeper potential well. It is only in cases where the tunneling matrix element is comparable to (or larger than) the asymmetry parameter that both wells will be populated. In such cases, the tunneling matrix element can be determined. This has been done for benzoic acid crystals doped with dye molecules. In that case, the asymmetry is reduced to about 1 cm^{-1} for the benzoic acid dimers that are nearest neighbor to a dye molecule.¹¹ The tunneling matrix element is found to be relatively independent of the nature of the dopant. For thioindigo-doped benzoic acid crystals, a

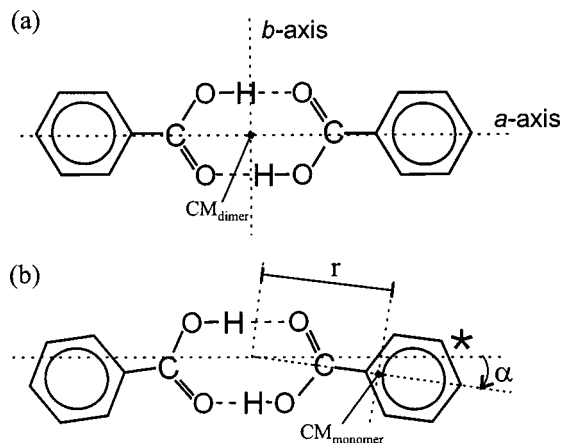


FIG. 1. The structure of the benzoic acid dimer in the ground (a) and electronically excited state (b). The star denotes the monomer unit that has been excited. Also shown in (b) are the definitions of the parameters that are used to characterize the structure of the benzoic acid dimer; α is the angle between the longitudinal axis of the dimer and that of the monomer unit, while r is the distance from the center of mass of the monomer unit to the center of rotation (i.e., the center of mass of the dimer having a linear configuration).

value of 8.4 GHz was found, while a value of 6.5 GHz was obtained if selenoindigo was the dopant.^{11,21} No value has been reported yet for the tunneling splitting in an isolated benzoic acid dimer. The benzoic acid monomer has been studied by microwave spectroscopy,²² but since the dimer is centrosymmetric it cannot be studied with the same technique.

Comparison of experimental results with theoretical studies shows that the proton transfer is strongly coupled to motion of the heavy nuclei, i.e., the whole benzoic acid frame rearranges itself slightly as the protons tunnel between the two benzoic acid units. From experimental results (activation energy and OH stretching vibration frequency), the potential barrier has been estimated⁴ to be 1850 cm^{-1} . In performing several *ab initio* calculations, geometry optimization of the transition state, a step which lowers the calculated potential barrier, was found to be necessary to reproduce the estimated potential barrier.^{4,23} This implies that a multidimensional potential is necessary to reproduce the observed features.^{24–27}

Very few studies on isolated benzoic acid dimers have been reported.^{28–31} For free dimers, the two constituents are equivalent and consequently the potential describing the proton tunneling is symmetric. The lowest singlet–singlet transition, $S_1 \leftarrow S_0$, is located at $35\,724\text{ cm}^{-1}$. This is a $\pi^* \leftarrow \pi$ transition, analogous to the ${}^1B_{2u} \leftarrow {}^1A_{1g}$ transition in benzene. Isotope studies show that the excitation is essentially localized in one of the monomer units.^{5,28} The two constituents are no longer equivalent after electronic excitation, thus the symmetry of the dimer is broken in S_1 . The potential for proton transfer will be given by an asymmetric potential, schematically given in Fig. 2(a). However, since no distinction can be made as to which of the two molecules in the dimer is excited, the symmetry in the potential surface must be restored. In general, the two potentials are coupled, which gives rise to a symmetric potential depicted in Fig.

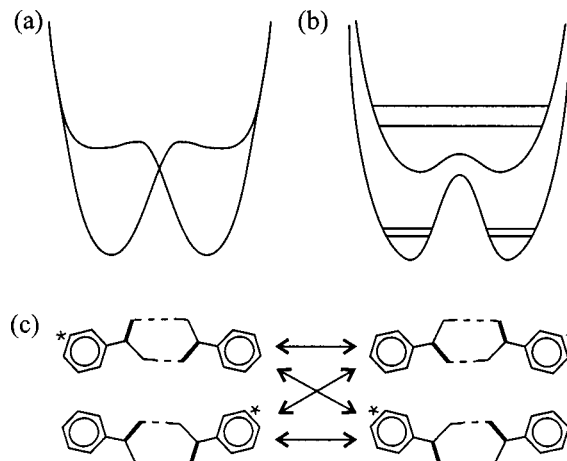


FIG. 2. The potential describing double proton transfer in the benzoic acid dimer. Localized excitation breaks the symmetry of the potential (a), but coupling between the two asymmetric potentials leads to two symmetric potentials (b). The coupling shown in (c) can be induced by excitation exchange (horizontal arrows) or by ν_3'' inversion (diagonal arrows).

2(b). This is similar to the description of the interconversion tunneling in $(\text{HF})_2$ and $(\text{HCCH})_2$ (Ref. 32) and of the tunneling dynamics in the ammonia dimer (Ref. 33).

The coupling in the benzoic acid dimer can be induced by exchange of the excitation from one unit to the other [see Fig. 2(c)]. Also inversion along the in-plane intermolecular ν_3'' coordinate can induce coupling between the two potentials. The localized excitation increases the basicity of the excited unit and decreases its acidity so that it will act as a proton acceptor, while the nonexcited unit will act as a proton donor. This causes the dimer to bend along the ν_3'' coordinate, as is shown in Fig. 1(b).^{5,30} As a result of the bend, an angular parameter is required (in addition to r) to characterize the structure of the dimer in the S_1 state. Here this parameter, denoted α , is taken to be the angle between the a -axis of the dimer and the a -axis of the excited monomer.

II. EXPERIMENT

A molecular beam in combination with a high resolution UV excitation source was used to measure the rotationally resolved fluorescence excitation spectrum of the benzoic acid dimer. The apparatus has been extensively described elsewhere.³⁴ In brief, the molecular beam is formed by flowing a carrier gas over the benzoic acid sample (Fluka), which is kept at 120°C . The beam is subsequently expanded through a 0.15 mm quartz nozzle, which is kept at a slightly higher temperature. In the expansion region, the dimers are formed. Neon rather than argon was used as the carrier gas. This choice was made to avoid consuming too high a percentage of the benzoic acid monomers in the formation of clusters with the carrier gas. At the same time, use of neon insures sufficient rotational cooling is achieved.

The molecular beam is skimmed twice in a differential pumping system and crosses the UV laser beam at right angles at about 30 cm from the nozzle. To insure collision-free conditions, the pressure in the detection chamber is kept

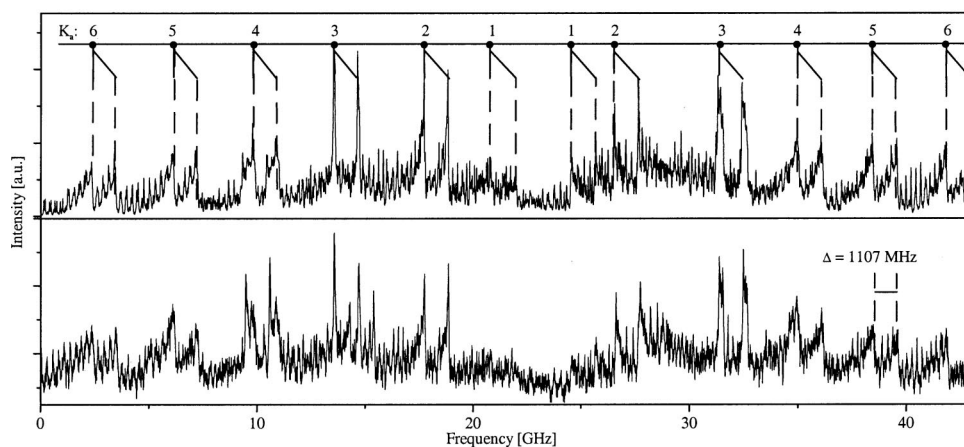


FIG. 3. The experimental spectrum of the benzoic acid dimer (lower panel), compared with a simulation using rotational constants that are calculated from rotational constants of the benzoic acid monomer (upper panel). The upper panel shows the labeling of the K_a -stacks.

below 10^{-6} mbar. The total undispersed fluorescence is imaged onto a photomultiplier, which is connected to a photon counting system interfaced with a computer.

UV radiation at 280 nm is generated by intracavity frequency doubling of a cw single frequency ring dye laser operating with Rhodamine 110. By using a 2 mm thick Brewster cut BBO crystal, 0.15 mW of tunable UV radiation is obtained with a bandwidth of 3 MHz. For relative frequency calibration, a temperature-stabilized Fabry–Perot interferometer with a free spectral range of 75 MHz is used. For absolute frequency calibration, the iodine absorption spectrum³⁵ was recorded simultaneously.

The resolution of the spectrometer is determined by the geometry of the fluorescence collection optics and by the residual Doppler width arising from the angular spread of the molecular beam. The latter depends on the carrier gas used to form the molecular beam, and is about 16 MHz when argon is used. Since neon is about twice as light as argon, we expect a Gaussian contribution to the linewidth of 23 MHz.

III. RESULTS

The high resolution UV excitation spectrum of the $S_1 \leftarrow S_0$ transition of the benzoic acid dimer is given in the lower panel of Fig. 3.

It can be clearly identified as a composite of two b -type components with selection rules $\Delta K_a = \pm 1$. The frequency separation between corresponding lines in the two components is here denoted by Δ (defined to be positive). This separation appears to be constant in the spectrum for all pairs of corresponding lines. As is shown in Fig. 4, the two tunneling states in the ground state potential have opposite parities; the same is true for the two tunneling states in the excited state potential. Each of the two b -type components arises from transitions originating in a different tunneling level of the ground state potential. Since the parity must change in an electric dipole transition, it is clear that the transitions for the two different components must also end on different tunneling states in the excited state potential. Consequently, if the energy ordering of the two parity levels in the ground and excited states is the same, as is the case for the higher energy transitions given in Fig. 4, then Δ will be the sum of the tunneling splittings in the two electronic

states. On the other hand, if the energy ordering is reversed, then Δ will be the difference of the tunneling splittings in the upper and lower electronic states. This is the case for the lower energy transitions in Fig. 4. Whether Δ is the sum or difference depends on the symmetry of the upper state (relative to that of the ground state).

To determine the value of Δ accurately, the autocorrelation of the spectrum is calculated using the correlation theorem.³⁶ The experimental spectrum is correlated with itself and the area of overlap between the two spectra is calculated as a function of the relative shift of the two spectra.³⁷ The autocorrelation spectrum, given in Fig. 5, shows three sharp maxima: at zero frequency shift, where the spectra overlap exactly, and at $+1107$ MHz as well as at -1107 MHz, where the frequency shift between the two components equals $+\Delta$ and $-\Delta$. From this analysis, it was determined that $\Delta = 1107 \pm 7$ MHz.

The observed excitation spectrum is very dense and no

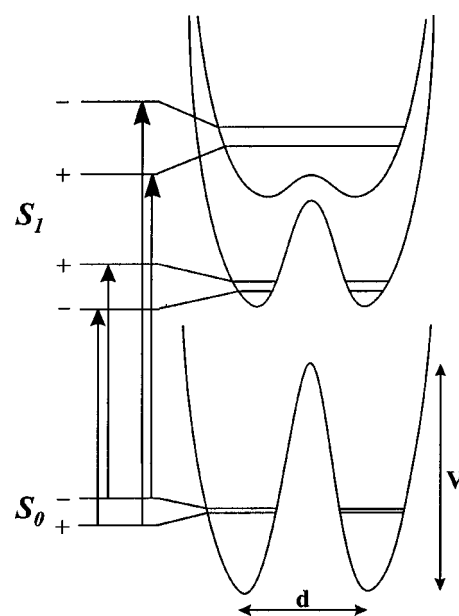


FIG. 4. Allowed transitions between tunneling levels in the ground and electronically excited state potentials. The parity has to change upon electronic excitation. For illustration purposes, parities as well as barrier heights (and tunneling splittings) are chosen arbitrarily.

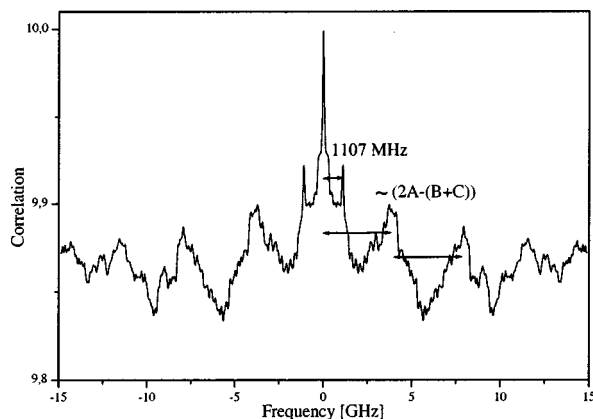


FIG. 5. The autocorrelation spectrum of the $S_1 \leftarrow S_0$ transition of the benzoic acid dimer. The spacing between the sharp peaks in the middle is the frequency separation Δ between corresponding transitions in the two different components that make up the spectrum. The separation between neighboring broad peaks is approximately equal to $[2A - (B + C)]$.

single transition can be distinguished. It is therefore impossible to make a full assignment of the spectrum and fit the rotational constants of the ground and the electronically excited state in the conventional manner. However, the spectrum shows some very characteristic features. In the autocorrelation spectrum, a series of broad peaks appear with an approximately constant spacing (see Fig 5). Each of these peaks is formed from a particular K -stack; that is, it is formed from a series of blended Q -branch transitions originating in ground state levels with the same K_a ; these transitions have the same value of ΔK_a . The spacing between K -stacks is approximately equal to $[2A - (B + C)]$, but it also depends weakly on ΔA . The width of each stack is determined by $\Delta(B + C)$. Throughout the spectrum, a number of lines can be found with an almost constant spacing corresponding to P and R branch transitions that originate from levels with the same K_a and have the same ΔK_a . The interval between these lines depends on $(B'' + C'')$ and $\Delta(B + C)$. Consequently, in spite of the fact that it is not possible to assign individual transitions in the spectrum, a great deal of information can be extracted. By comparing the experimental spectrum with spectra simulated for various values of the molecular parameters, a range of acceptable values has been determined for each rotational constant except for ΔB and ΔC , for which a value for the sum $\Delta(B + C)$ has been determined instead. The results for the rotational constants are given in Table I. The origin of the transition that has the lowest frequency has been determined at $35\,723.82 \pm 0.05$ cm^{-1} .

By using the experimental results in Table I and the rotational constants of the monomer as determined by microwave spectroscopy,²² values for r and α can be estimated for both the S_0 and S_1 states and considerable insight into the structure can be obtained.

As was indicated in Sec. I, the ground state is assumed to be linear. The value of r can be determined from its effects on B'' and C'' ; from the values of these constants given in Table I it was found that $r = 3.622 \pm 0.147$ Å. This result is in very good agreement with the value for r of 3.58 Å deduced

TABLE I. Rotational constants of the benzoic acid dimer in the ground and electronically excited state. The calculated constants are determined for a linear configuration with $r = 3.58$ Å in the ground state and a bent configuration with $\alpha = 3.4^\circ$ and $r = 3.60$ Å in the excited state. See text. All values are given in MHz.

		Experimental	Calculated
S_0 -state	A''	1923(16)	1928.9
	B''	127(8)	127.9
	C''	114(8)	120.0
S_1 -state	ΔA	-15(10)	-12.48
	$\Delta(B + C)$	-1.5(7)	-1.16

from the $\text{O} \cdots \text{O}$ distance determined by Brougham *et al.*¹⁷ In order to check the linearity of the ground state, the angle α defined in Fig. 1 was varied. If the rotational constants for the S_0 state are to be consistent with those given in Table I, then the dimer cannot be bent by more than 5.1° in the ground state.

For the excited state, a bent structure has been suggested.^{5,30} For this state, both r and α were varied. As compared to the ground state values, both parameters must be increased in order to reproduce the experimental determinations of the rotational constants. The larger α is in the ground state, the smaller is the increase required in α upon electronic excitation.

If a linear ground state is assumed, then the excited state value of α must fall in the range from 1.7° to 5.1° in order to obtain rotational constants that are in agreement with those given in Table I. The value of r increases by from 0.01 to 0.03 Å.

Very good agreement with the experimental spectrum is obtained for a linear ground state structure with r equal to 3.58 Å and an excited state structure that is bent by 3.4° with a distance r of 3.60 Å. The rotational constants that are calculated from these structures are given in Table I, while the upper part of Fig. 3 shows a simulation using these constants.

IV. CONCLUSION

The experimental spectrum of the benzoic acid dimer clearly reveals a tunneling splitting due to proton transfer in the ground and electronically excited state. A spectrum consisting of two rigid rotor components is found with a splitting of $\Delta = 1107 \pm 7$ MHz. No gas phase measurements of the tunneling splittings in the benzoic acid dimer have been previously reported. The tunneling matrix element for the ground state of benzoic acid crystals doped with different dye molecules was determined to be 8.4 GHz and 6.5 GHz, respectively.^{11,21} If these values are used as an estimate of the tunneling splitting in the ground state of the isolated dimer, the frequency separation Δ equals the difference in the tunneling splittings in the ground and electronically excited states. It follows that transitions are made between the lower tunneling level in the ground state potential and the lower tunneling level in the excited state potential. (Upper-to-upper transitions form the other component of the spectrum.) This can occur only if the energy ordering of the two

parity levels in the excited state is inverted as compared to the ordering in the ground state. If it is further assumed that the tunneling path and effective tunneling mass do not change upon excitation, the value of 1107 MHz for Δ implies a change in the potential barrier of about 20% upon electronic excitation. It is not known whether the barrier increases or decreases. Only an absolute value for Δ has been determined from the spectrum. In case the barrier in the excited state is smaller than in the ground state (i.e., the tunneling splitting in the excited state is larger than in the ground state), the lower frequency component in the spectrum corresponds to the lower-to-lower transitions and the higher frequency component to the upper-to-upper transitions, whereas if the barrier in the excited state is larger the lower frequency component in the spectrum corresponds to the upper-to-upper transitions.

The simulated spectrum using calculated rotational constants is in good agreement with the measured spectrum. For the ground electronic state, it is concluded that the dimer has a linear structure with r equal to 3.58 Å, yielding a distance of 7.16 Å between the centers of mass of the two monomers. For the excited electronic state, it is concluded that the dimer is bent by about 3.4° with r being equal to 3.60 Å.

It would be very interesting to see how the tunneling splitting evolves in the different vibrational modes of the dimer, especially in the bending mode ν_3'' , which is expected to couple efficiently to the proton tunneling. Such measurements are currently on the way in our laboratory.

ACKNOWLEDGMENTS

Authors would like to thank Professor Dr. Gerard Meijer for suggesting this experiment. This work was made possible by funding from the Dutch Foundation for Fundamental Research on Matter (FOM). One of us (I.O.) would like to thank the University of Nijmegen for its hospitality during the period November 1997 to February 1998.

¹H. Morita and S. Nagakura, *J. Mol. Spectrosc.* **42**, 536 (1972).

²C. C. Costain and G. P. Srivastava, *J. Chem. Phys.* **41**, 1620 (1964).

³G. Allen, J. G. Wathinson, and K. H. Webb, *Spectrochim. Acta* **22**, 807 (1966).

⁴S. Nagaoka, N. Hirota, T. Matsushita, and K. Nishimoto, *Chem. Phys. Lett.* **92**, 498 (1982).

⁵J. C. Baum and D. S. McClure, *J. Am. Chem. Soc.* **102**, 720 (1980).

⁶S. Nagaoka, T. Terao, F. Imashiro, A. Saika, and N. Hirota, *J. Chem. Phys.* **79**, 4694 (1983).

⁷J. M. Clemens, R. M. Hochstrasser, and H. P. Trommsdorff, *J. Chem. Phys.* **80**, 1744 (1984).

⁸G. R. Holtom, H. P. Trommsdorff, and R. M. Hochstrasser, *Chem. Phys. Lett.* **131**, 44 (1986).

⁹R. M. Hochstrasser and H. P. Trommsdorff, *Chem. Phys.* **115**, 1 (1987).

¹⁰C. Rambaud, A. Oppenländer, M. Pierre, H. P. Trommsdorff, and J. Vial, *Chem. Phys.* **136**, 335 (1989).

¹¹A. Oppenländer, C. Rambaud, H. P. Trommsdorff, and J. Vial, *Phys. Rev. Lett.* **63**, 1432 (1989).

¹²A. Stöckli, B. H. Meier, R. Kreis, R. Meyer, and R. R. Ernst, *J. Chem. Phys.* **93**, 1502 (1990).

¹³A. J. Horsewill, P. J. McDonald, and D. Vijayaraghavan, *J. Chem. Phys.* **100**, 1889 (1994).

¹⁴S. G. Stepanian, I. D. Reva, E. D. Radchenko, and G. G. Sheina, *Vib. Spectrosc.* **11**, 123 (1996).

¹⁵C. Scheurer and P. Saalfrank, *Chem. Phys.* **104**, 2869 (1996).

¹⁶C. C. Wilson, N. Shankland, and A. J. Florence, *Chem. Phys. Lett.* **253**, 103 (1996).

¹⁷D. F. Brougham, A. J. Horsewill, A. Ikram, R. M. Ibberson, P. J. McDonald, and M. Pinter-Krainer, *J. Chem. Phys.* **105**, 979 (1996).

¹⁸D. F. Brougham, A. J. Horsewill, and R. I. Jenkinson, *Chem. Phys. Lett.* **272**, 69 (1997).

¹⁹J. Seliger and V. Žagar, *Chem. Phys.* **234**, 223 (1998).

²⁰M. Neumann, D. F. Brougham, C. J. McGloinn, M. R. Johnson, A. J. Horsewill, and H. P. Trommsdorff, *J. Chem. Phys.* **109**, 7300 (1998).

²¹Ch. Rambaud and H. P. Trommsdorff, *Chem. Phys. Lett.* **306**, 124 (1999).

²²M. Onda, M. Asai, K. Takise, K. Kuwae, K. Hayami, A. Kuroe, M. Mori, H. Miyazaki, N. Suzuki, and I. Yamaguchi, *J. Mol. Struct.* **482–483**, 301 (1999).

²³F. Graf, R. Meyer, T. -K. Ha, and R. R. Ernst, *J. Chem. Phys.* **75**, 2914 (1981).

²⁴R. Meyer and R. R. Ernst, *J. Chem. Phys.* **93**, 5518 (1990).

²⁵C. Scheurer and P. Saalfrank, *Chem. Phys. Lett.* **245**, 201 (1995).

²⁶V. P. Sakun, M. V. Vener, and N. D. Sokolov, *J. Chem. Phys.* **105**, 379 (1996).

²⁷D. Antoniou and S. D. Schwartz, *J. Chem. Phys.* **109**, 2287 (1998).

²⁸D. E. Poeltl and J. K. McVey, *J. Chem. Phys.* **78**, 4349 (1983).

²⁹Y. Tomioka, H. Abe, N. Mikami, and M. Ito, *J. Phys. Chem.* **88**, 2263 (1984).

³⁰D. E. Poeltl and J. K. McVey, *J. Chem. Phys.* **80**, 1801 (1984).

³¹G. Meijer, M. S. de Vries, H. E. Hunziker, and H. R. Wendt, *J. Phys. Chem.* **94**, 1801 (1990).

³²G. T. Fraser, *J. Chem. Phys.* **90**, 2097 (1989).

³³H. Linnartz, W. L. Meerts, and M. Havenith, *Chem. Phys.* **193**, 327 (1995).

³⁴W. A. Majewski and W. L. Meerts, *J. Mol. Spectrosc.* **104**, 271 (1984).

³⁵S. Gerstenkorn and P. Luc, *Atlas du Spectroscopie d'Absorption de la Molécule d'Iode* (CNRS, Paris, 1978); *Rev. Phys. Appl.* **14**, 791 (1979).

³⁶W. H. Press, S. A. Teukolsky, W. T. Vetterling, and B. P. Flannery, *Numerical Recipes in C: The Art of Scientific Computing* (Cambridge University Press, Cambridge, 1992).

³⁷R. M. Helm, H. P. Vogel, and H. J. Neusser, *Chem. Phys. Lett.* **270**, 285 (1997).